Medición de los decaimientos del bosón de Higgs en el FCC-ee a $\sqrt{s} = 240$ GeV y $\sqrt{s} = 365$ GeV

3° Taller en Automatización de Cálculos en Física de Partículas - CIIEC

J. Eysermans[★], **Haydee Hernández-Arellano**[†], F. Martínez[†], I. Pedraza[†]

[†]Benemérita Universidad Autónoma de Puebla
Puebla, Puebla, México.
[★]Massachusetts Institute of Technology,
Cambridge, Massachusetts, USA.

November 19, 2025

Outline

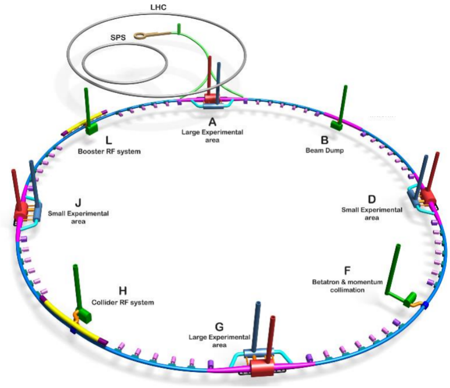

LHC
SPS
A
Large Experimental area
B
Beam Dump
D
Small Experimental area
F
Betatron & momentum collimation
G
Large Experimental area
H
Collider RF system
J
Small Experimental area
L
Booster RF system

Standard Model

- Quantum Field Theory: Electromagnetic + Weak + Strong Forces
- Symmetry group: $SU(3)_C \otimes SU(2)_L \otimes U(1)_Y$
- Self-consistent. Free of anomalies. Consistent perturbative scheme for systems at very high energies (LHC at 13 TeV)
- Higgs: last piece of the theory discovered in 2012, $M_H = 125\ GeV$.

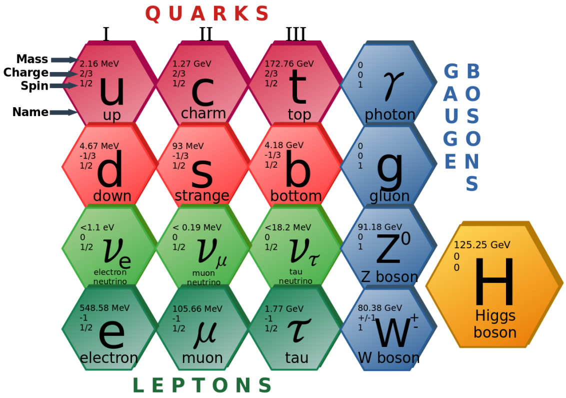

Importance of the Higgs

- SM $\rightarrow$ Quantum Field Theory as basis for Electromagnetism
- Same approach for Weak interactions $\rightarrow$ W and Z had to be massless!
- Brout-Englert-Higgs mechanism $\rightarrow$ Spontaneous Symmetry Breaking $\rightarrow$ W and Z acquire mass through the Higgs field.
- Fermions can also acquire mass the same way!

Why measure the Higgs properties with high precision?

- The Higgs boson as a light scalar leads to a Hierarchy problem $\rightarrow$ Sensitive to larger scales!
- Electroweak Phase transition
- Higgs portal to Dark Matter?

Search for the Higgs at Colliders

1989–2000

Large Electron Positron (LEP)
CERN

- e^+e^- collider
- $\sqrt{s} = 189$–209 GeV
- $L_{int} \sim 600$ pb^{-1}
- $m_H > 114.4$ GeV$/c^2$

→

2001–2011

Tevatron
Fermilab

- $p\bar{p}$ collider
- $\sqrt{s} = 1.96$ TeV
- $L_{int} = 10$ fb^{-1}
- 3σ excess at 115–140 GeV$/c^2$

→

2009–present

Large Hadron Collider
CERN

- $p\bar{p}$ collider
- $\sqrt{s} = 13$–13.6 TeV
- $L_{int} = 29$ fb^{-1} at $\sqrt{s}$ =7-8 TeV (Run 1)
- $L_{int} > 400$ fb^{-1} (Run2+Run3)
- Discovery: $m_H = 125$ GeV$/c^2$

- LEP established the lower mass bound for the Higgs boson
- Tevatron observed a 3σ excess hinting at the Higgs
- LHC confirmed the discovery at $m_H = 125$ GeV$/c^2$ (2012)

Future Higgs Factories

A new generation of e^+e^- colliders is planned to act as "Higgs Factories" for high-precision measurements.

Table: Comparison of future e^+e^- Higgs factories.

Feature	**FCC-ee**	**CEPC**	**ILC**	**CLIC**
Type	Circular	Circular	Linear	Linear
Circumference/Length	100 km	100 km	20 km	48 km
Center of Mass Energy Range	88-365 GeV	90-240 GeV	250-500 GeV	380 GeV-3 TeV
Key Technology	Crab-waist	Double RF	SCRF Cavities	Two-beam Accel.
Higgs/Year (@240 GeV)	1.2 Million	1.0 Million	140k	N/A

HL-LHC Prospects

Start of operations: June 2030

Phase 1: $\sqrt{s} = 14$ TeV, $L_{int} = 3$ ab^{-1}

Potential upgrade: $\sqrt{s} \rightarrow 27$ TeV (HE-LHC), $L_{int} = 15$ ab^{-1}

Enhanced Higgs Physics Program:

- Search for rare decays: $H \rightarrow \mu^+\mu^-$, $H \rightarrow c\bar{c}$, $H \rightarrow Z\gamma$
- Di-Higgs production: $\sim$100,000 events expected
- Constrain Higgs trilinear coupling λ_{HHH}

The HL-LHC will transform Higgs physics from discovery era to precision measurements, opening new windows to rare processes and fundamental Higgs properties.

Linear vs Circular Colliders

Linear Colliders (ILC, CLIC)	Circular Colliders (HL-LHC, FCC)
Advantages	
▪ Higher center of mass energy capability	▪ Higher luminosity achieved
▪ Avoids synchrotron radiation losses	▪ Beam re-use enables high statistics
▪ Ideal for heavy particle searches and high-energy processes	▪ Excellent for precision measurements and rare decay studies
Limitations	
▪ Limited luminosity	▪ Energy limited by synchrotron losses
▪ Single-pass beam operation	▪ Large physical footprint required
▪ Lower event statistics	▪ Higher infrastructure costs

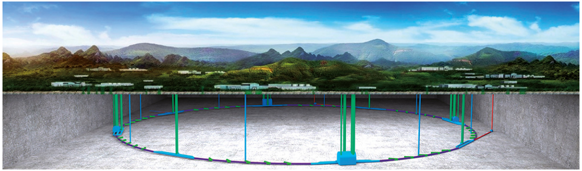

Circular Electron-Positron Collider (CEPC)

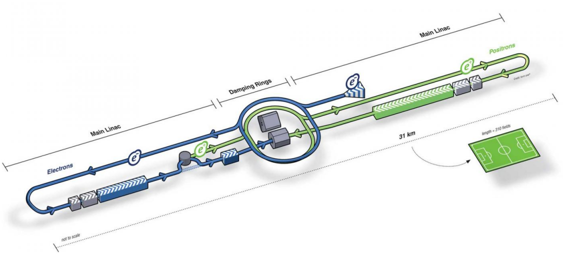

Internacional Linear Collider

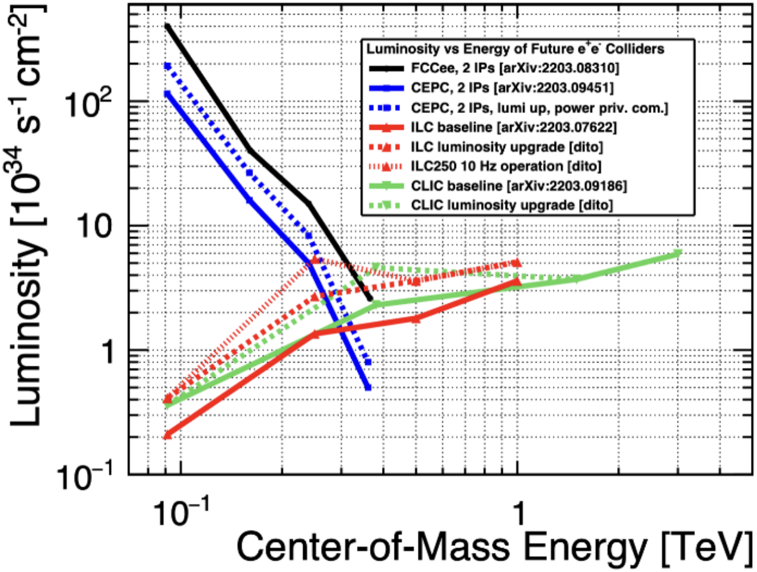
Luminosity vs Energy of Future e+e- Colliders
FCCee, 2 IPs [arXiv:2203.08310]
CEPC, 2 IPs [arXiv:2203.09451]
CEPC, 2 IPs, lumi up, power priv. com.]
ILC baseline [arXiv:2203.07622]
ILC luminosity upgrade [dito]
ILC250 10 Hz operation [dito]
CLIC baseline [arXiv:2203.09186]
CLIC luminosity upgrade [dito]
Luminosity [10^{34} s^{-1} cm^{-2}]
10^2
10
1
10^{-1}
10^{-1}
1
Center-of-Mass Energy [TeV]

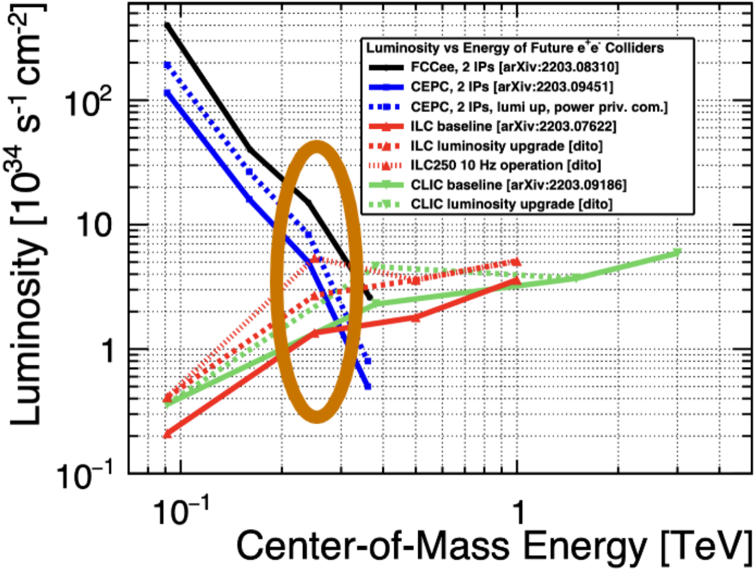

Luminosity vs Energy of Future e+e- Colliders
FCCee, 2 IPs [arXiv:2203.08310]
CEPC, 2 IPs [arXiv:2203.09451]
CEPC, 2 IPs, lumi up, power priv. com.]
ILC baseline [arXiv:2203.07622]
ILC luminosity upgrade [dito]
ILC250 10 Hz operation [dito]
CLIC baseline [arXiv:2203.09186]
CLIC luminosity upgrade [dito]
Luminosity [10^{34} s^{-1} cm^{-2}]
Center-of-Mass Energy [TeV]

FCC Proposal

The **Future Circular Collider** surges as a response to the 2013 European Strategy for Particle Physics Update (ESPPU), where an "*ambitious post-LHC accelerator project at CERN*" was requested.

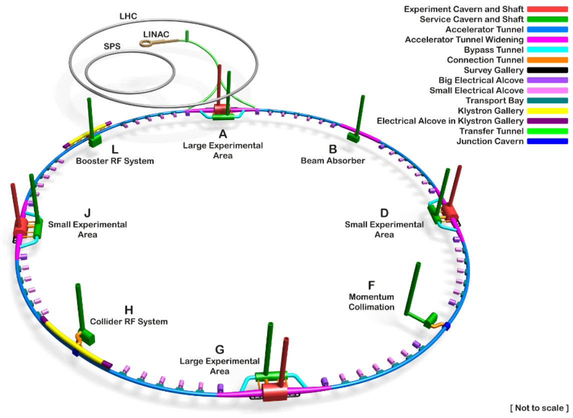

FCC opportunities*

.

- Map **Higgs and EW gauge boson properties** with unprecedented precision, probing interactions linked to the early universe ($10^{-12} - 10^{-10}$ s after the Big Bang).
- Improve knowledge of Standard Model phenomena (EW, QCD, flavour, Higgs, top) through **high-precision measurements**.
- Boost sensitivity to **rare low-energy processes**, including light, weakly coupled particles (e.g., neutrinos, axion-like particles), and decisively test dark matter candidates.
- Extend direct discovery reach for **new particles** by at least an order of magnitude at high energies.

*See more information at the **Future Circular Collider Feasibility Study Report**: Volume 1, Physics, Experiments, Detectors. DOI: 10.17181/CERN.9DKX.TDH9.

FCC-ee and FCC-hh

FCC-ee
$\sqrt{s} = 88 - 365$ GeV

$\rightarrow$

~ 3 million Higgs
Probe Higgs mass, width, and couplings

FCC-hh
up to $\sqrt{s} = 100$ TeV

$\rightarrow$

~ 20 billion Higgs
Probe Higgs self-coupling, top Yukawa, and other rare and invisible modes

FCC-ee baseline luminosity

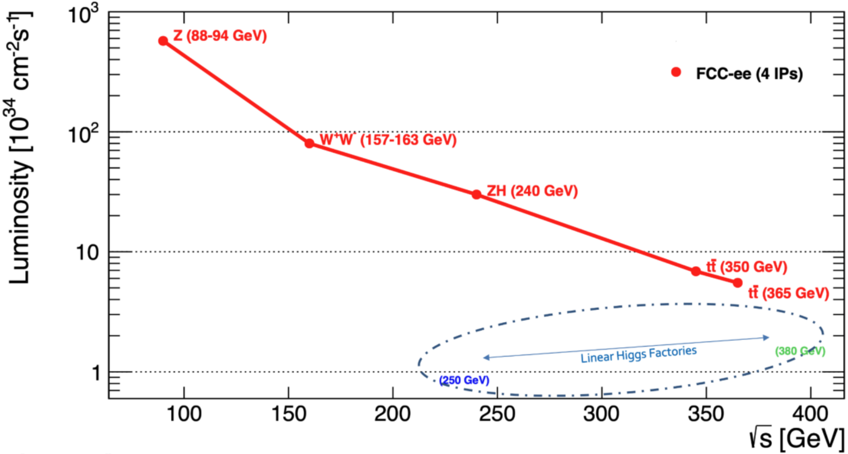

The FCC-ee baseline design luminosity, summed over 4 IPs, displayed as a function of the center-of-mass energy, from the Z pole to the tt threshold and beyond (from **FCC Feasibility Study Report**).

FCC-ee baseline integrated luminosity

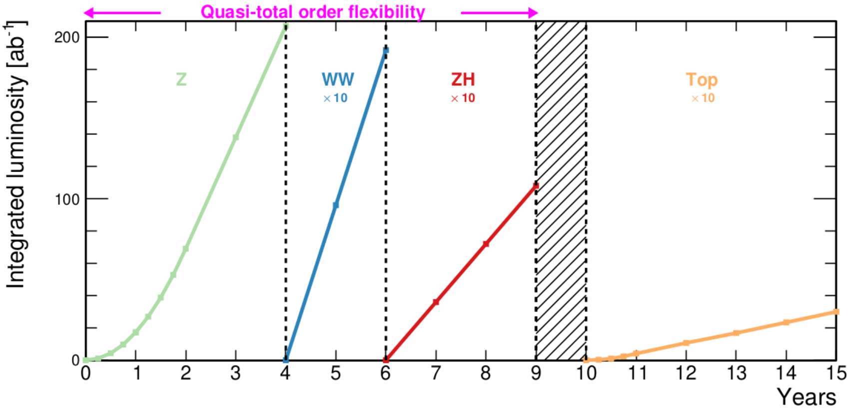

The FCC-ee baseline model of operation, and integrated luminosity as a function of time (from **FCC Feasibility Study Report**).

Higgs production from e^+e^- colliders at $\sqrt{s} = 240$ GeV

In e^+e^- collisions at $\sqrt{s} = 240$ GeV, Higgs are mainly produced through two modes: "Higgsstrahlung" and WW fusion process (VBF):

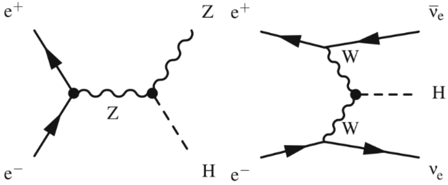

Higgs production modes for e^+e^- colliders at $\sqrt{s} = 240$ GeV *.

At the FCC-ee: significantly larger number of ZH events with a much smaller background will be observed compared with previous observations by ATLAS and CMS.

*Eysermans, J., & Selvaggi, M. (2025). DOI: 10.17181/9gzts-hsm97

Higgsstrahlung

Higgs model-independent studies can be carried out in Higgsstrahlung events: center-of-mass is known, information on the recoiling Higgs is accessible by the associated Z boson *.

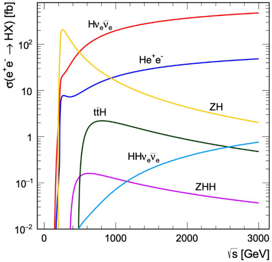

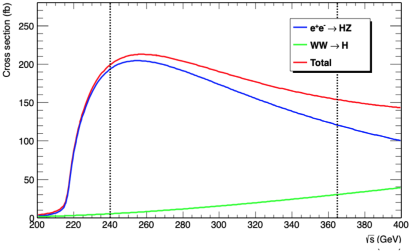

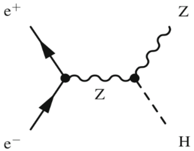

At $\sqrt{s} = 240$ GeV, the ZH rate is enhanced, sensitive to the eeZ and the ZZH vertices, along with the couplings to the Higgs. Images from: Sally Dawson, ZH at one loop in SMEFT

*Eysermans, J., Bernardi, G., Ang, L. (2025). DOI: 10.17181/jfb44-s0d81

Higgs couplings

From the Higgsstrahlung and WW fusion processses we can extract the different couplings of various Higgs decay modes ($H \to X\bar{X}$) using the following relations*:

$$
\begin{aligned}
\sigma_{ZH} \times Br(H \to X\bar{X}) &\propto \frac{g_{HZZ}^2 g_{HXX}^2}{\Gamma_H} \\
\sigma_{H\nu_e\nu_e} \times Br(H \to X\bar{X}) &\propto \frac{g_{HWW}^2 g_{HXX}^2}{\Gamma_H}
\end{aligned}
\tag{1}
$$

By analyzing the $H \to ZZ$ decay, we can extract the g_{HZZ} coupling from the first equation, which can then be used to obtain all other Higgs couplings for other decay channels.

*Eysermans, J., Bernardi, G., Ang, L. (2025). DOI: 10.17181/jfb44-s0d81

Other opportunities

Apart from determining the Higgs couplings with great precission, studying the ZH process will allow to

- Constraint the Higgs total width, by measuring the $H \to ZZ^*$ decay and the relation:

$$\Gamma_H \propto \frac{\sigma(e^+e^- \to ZH, H \to ZZ)^2}{\sigma(e^+e^- \to ZH}$$

- Probe the Higgs self-coupling through NLO deviations*:

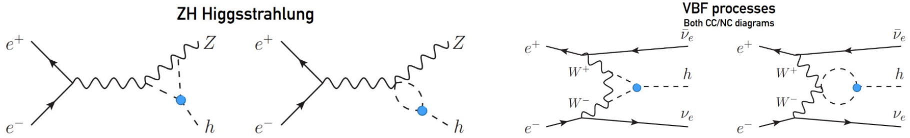

*Eysermans, J., Selvaggi, M. (2025) DOI:10.17181/9gzts-hsm97

$Z(\ell\ell)$ and $H \to WW$

- **Leptonic decays** of the Z boson $\to$ greater precision and efficient selection of the ZH events, independently of the Higgs decay mode[a].
- Our study will focus on the $H \to W^+W^-$ decay, particularly the **hadronic channel** ($\Gamma_{W,hadrons}/\Gamma_W \sim 67\%$).

[a]Eysermans, J., Bernardi, G., Ang, L. (2025). DOI: 10.17181/jfb44-s0d81

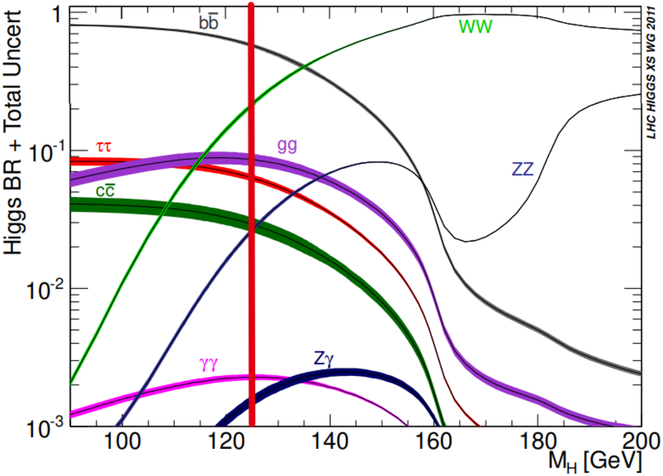

From: *Handbook of LHC Higgs Cross Sections*, DOI: 10.5170/CERN-2012-002

Recoil Mass Method

With a focus on the leptonic decays of the Z, the mass recoiling against the Z-lepton pair can be written as

$$m_{recoil}^2 = (\sqrt{s} - E_{\ell\ell})^2 - p_{\ell\ell}^2 = s - 2E_{\ell\ell}\sqrt{s} + m_{\ell\ell}^2. \tag{2}$$

Important points:

- The center-of-mass is chosen to maximize ZH production ($\sqrt{s} = 240$ GeV), 15 GeV below the σ_{ZH} maximum.
- The choice of $Z(\ell\ell)$ channel allows for model-independent determination of the g_{HZZ}, but it is statistically expensive.
- In absence of Beam Energy Spread (BES) and Initial State Radiation (ISR), $\sqrt{s}$ is well known and the m_{recoil} **coincides with the Higgs mass**.

Recoil Mass Method

- Main backgrounds: WW, ZZ and $Z\gamma$.
- m_{recoil} distribution shows two prominent peaks: one at m_Z from the ZZ process and one around 125 GeV, from the ZH process.

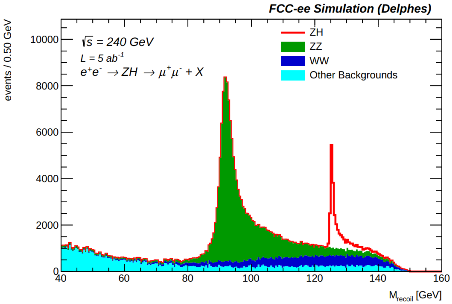

m_{recoil} after basic selection of two muons with invariant mass close to m_Z and total transverse momentum between 15 and 70 GeV*.

*Eur.Phys.J.Plus 137 (2022) 1, 23

Monte Carlo samples

- **I**nnovative **D**etector for an **E**lectron-positron **A**ccelerator, is a concept detector designed specifically for FCC-ee.
- Detector simulation and reconstruction performed using DELPHES.
- Monte Carlo event samples generated with either WHIZARD or PYTHIA8 (winter2023 campaign).
- $\sqrt{s} = 240$ GeV, and luminosity set at 10.8 ab^{-1}, with a BES of 0.185%.

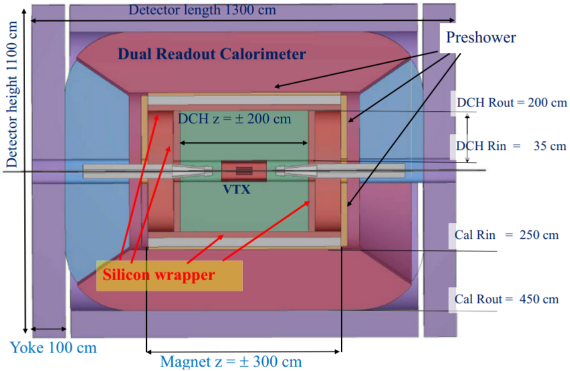

IDEA detector layout [a].

[a] Eur. Phys. J. Special Topics 228, 261–623 (2019)

Main backgrounds

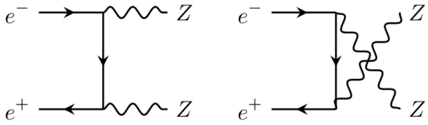

$e^+e^- \to ZZ.$

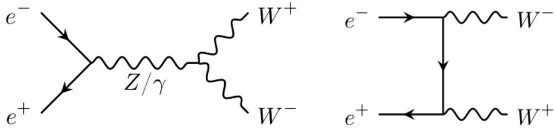

$e^+e^- \to W^+W^-.$

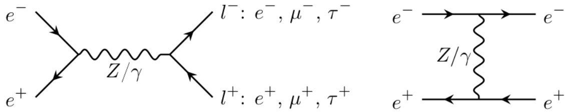

$e^+e^- \to \ell^+\ell^-$.

Other backgrounds

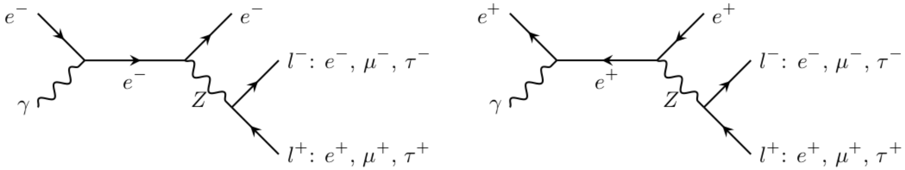

$e^-\gamma \to e^- Z(\ell^+\ell^-)$ and $e^+\gamma \to e^+ Z(\ell^+\ell^-)$.

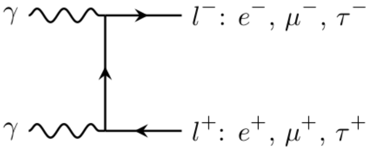

$\gamma\gamma \to \ell^+\ell^-$.

Final State of the Studied Process

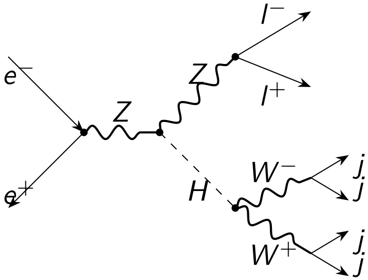

$e^+e^- \to Z(l^+l^-)H(W^+W^-)$

We study the process $e^+e^- \to ZH \to Z(\ell^+\ell^-)H(W^+W^-) \to Z(\ell^+\ell^-)W(qq)W(qq)$.

For the final state we look for events with:

1. Two opposite-charged electrons/muons.
2. At least one isolated, with p>20 GeV.
3. Four jets.

Signal and Background Samples

Process	Simulation Label	$\sigma[fb]$	Events Generated
Signal:			
$e^+e^- \to Z(\mu\mu)H,\ H \to WW$	wzp6_ee_mumuH_HWW_ecm240	1.456	400,000
$e^+e^- \to Z(ee)H,\ H \to WW$	wzp6_ee_eeH_HWW_ecm240	1.541	400,000
Background:			
$e^+e^- \to ZZ$	p8_ee_ZZ_ecm240	1358.99	11,300,000
$e^+e^- \to WW$	p8_ee_WW_ecm240	16438.5	74,728,800
$e^+e^- \to Z(\mu\mu)\gamma$	wzp6_ee_mumu_ecm240	5288	10,700,000
$e^+e^- \to ee$	wzp6_ee_ee_Mee_30_150_ecm240	8305	85,400,000
$e^+e^- \to Z(\mu\mu)H,\ H \to ZZ$	wzp6_ee_mumuH_HZZ_ecm240	0.1786	400,000
$e^+e^- \to Z(ee)H,\ H \to ZZ$	wzp6_ee_eeH_HZZ_ecm240	0.1891	400,000
$e^+e^- \to Z(qq)H,\ H \to ZZ$	wzp6_ee_qqH_HZZ_ecm240	1.409	1,200,000
$e^+e^- \to Z(bb)H,\ H \to ZZ$	wzp6_ee_bbH_HZZ_ecm240	0.7915	1,000,000
$e^+e^- \to Z(cc)H,\ H \to ZZ$	wzp6_ee_ccH_HZZ_ecm240	0.6164	1,200,000
$e^+e^- \to Z(ss)H,\ H \to ZZ$	wzp6_ee_ssH_HZZ_ecm240	0.7912	600,000

FCC Physics Events Samples

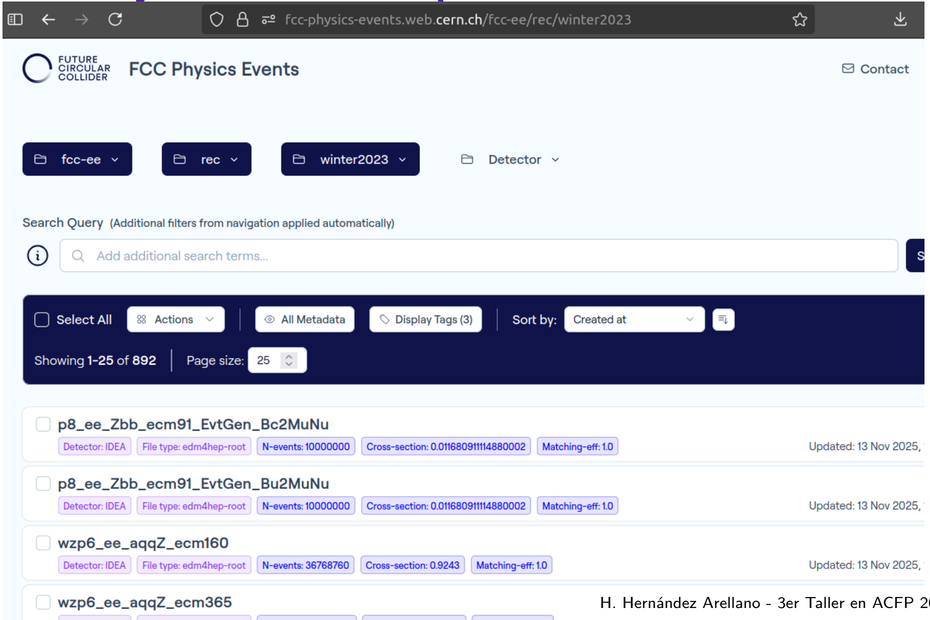

FCC Physics Events Samples

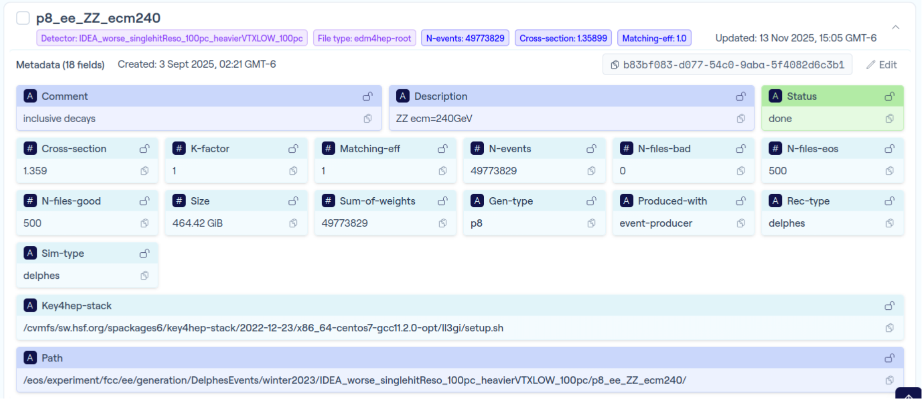

FCC Framework

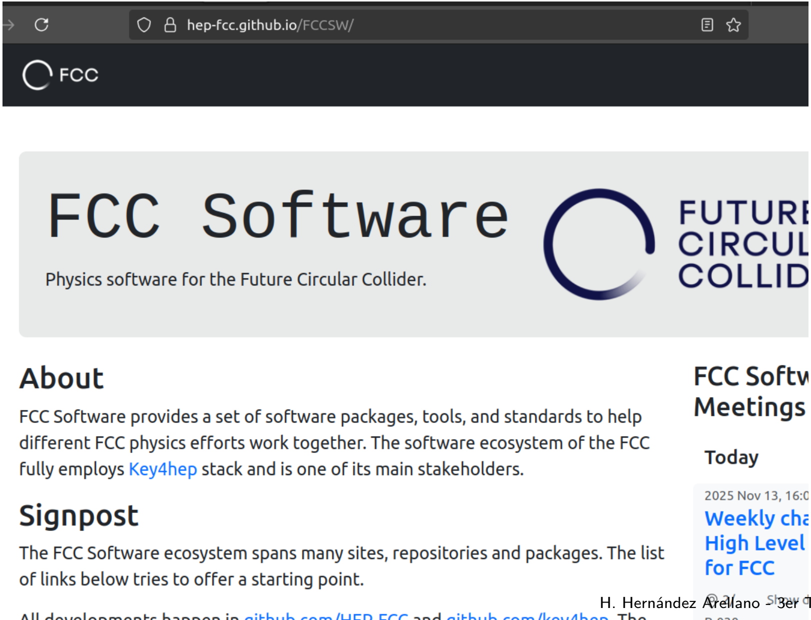

FCC Framework

1.1.4.2. Using a virtual machine through VirtualBox

The CernVM project provides a convenient tool to start VMs, cernvm-launch, and a public repository of contexts to be used with `cernvm-launch` to configure the VM at your needs. The tool `cernvm-launch` is available for Linux, Mac and Windows. A context dedicated to the FCC tutorials is available in the repository. The cernvm-launch works with VirtualBox, virtualization manager available for free for all platforms.

If you have a CERN account, this is a convenient way to enable access to the EOS storage system.

To create and use a CernVM virtual machine for the FCC tutorials please follow the following steps:

- Make sure VirtualBox is installed (details installing instructions from the product web page).
- Download the `cernvm-launch` binary for your platform either from the dedicated download page or from the following links:
  - Linux
  - Mac
  - Win

  Make sure is visible in your $PATH.
- Get the fcc-tutorial.context (use wget or curl)

$Z(l^+l^-)H$ event selection: kinematic cuts

1. 2 op. ch. muons, $p > 20$ GeV, at least one isolated
2. Veto on ℓ's with $5 < p < 20$ GeV
3. $m_{\ell\ell} \in [86, 96]$ GeV, $p_{\ell\ell} \in [30, 57]$ GeV
4. $|\cos\theta_{miss}| < 0.98$

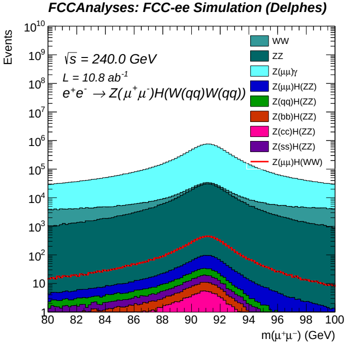

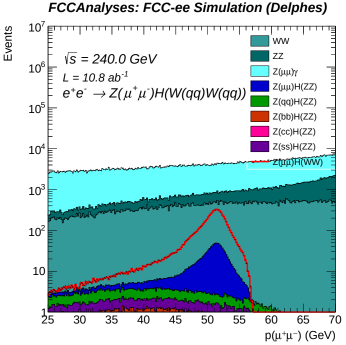

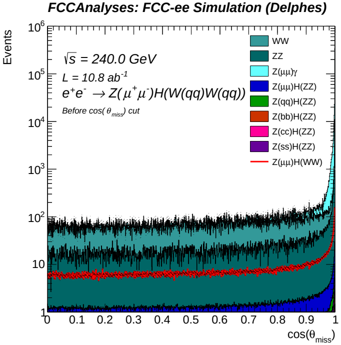

Jet Clustering and Di-Jet Pair Selection

- Restrict the $W \to \ell\nu$ decays by cuting events with missing energy $E_{miss} > 10$ GeV.
- Create a collection of particles removing both muons and electrons with $p > 20$ GeV.
- Exclusive $N = 4$ “Durham” algorithm is used for jet clustering, which is a sequential spherical k_t clustering method[a].

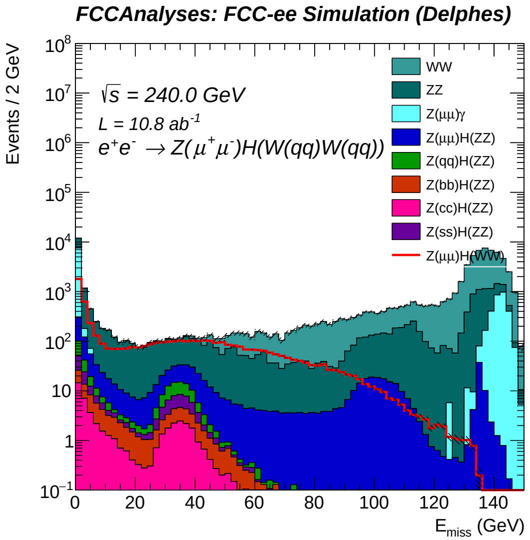

[a] S. Catani et al Physics Letters B, 269(3):432–438, 1991

Jet Clustering and Di-Jet Pair Selection

We choose the best dijet pair to reconstruct the two W bosons by maximizing[a] :

$$P_W^{jj} = \frac{M_W^2 \Gamma_W^2}{\left(m_{jj}^2 - M_W^2\right)^2 + M_W^2 \Gamma_W^2}. \qquad (3)$$

- $jj[0]$: Maximizing pair (*"on-shell"*).
- $jj[1]$: The remaining pair (*"off-shell"*).

Same procedure but with M_Z and Γ_Z instead: use the resulting dijet-pair invariant mass ($m^Z_{jj[0]}$) to further reduce the ZZ background.

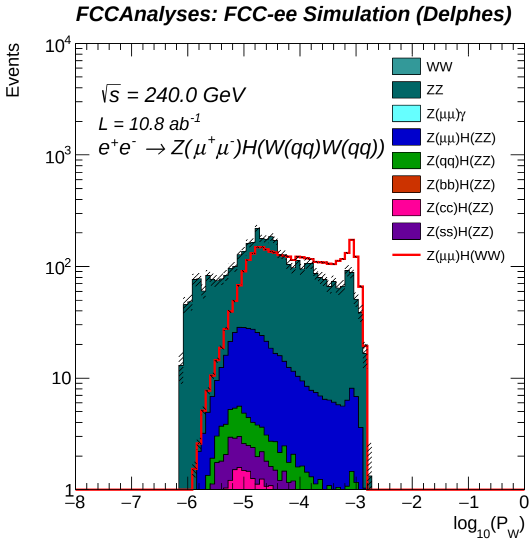

[a]Piotr Niezurawski et al JHEP11(2002)034

Di-jet pair invariant mass

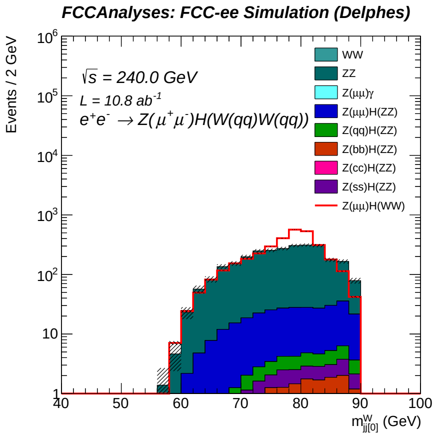

"On-shell" W di-jet pair invariant mass.

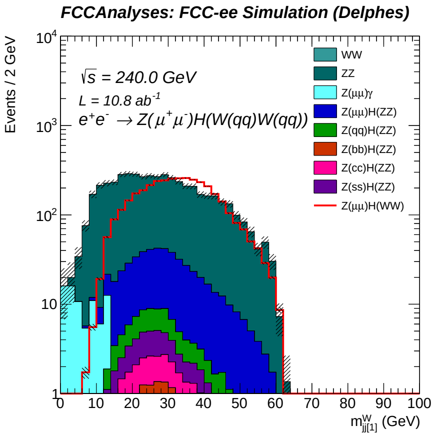

"Off-shell" W di-jet pair invariant mass.

Final Selection Cuts

- Cut 1: Events with only two opposite charge $\mu's$.
- Cut 2: Veto on $\mu's$ and $e's$ with momentum within $[5, 20]$ GeV.
- Cut 3: $86 < m_{\mu\mu} < 89$ GeV.
- Cut 4: $30 < p_{\mu\mu} < 57$ GeV.
- Cut 5: $|\cos\theta_{miss}| < 0.98$.
- Cut 6: Missing energy $E_{miss} < 10$ GeV.
- Cut 7: $n_{jet} = 4$.
- Cut 8: $125 < E^{\text{no Z}}_{visible} < 145$ GeV, where $E^{\text{no Z}}_{visible}$ is the visible energy of the particles excluding the two Z muons.
- Cut 9: $120 < m_{4j} < 130$ GeV, where m_{4j} is the four-jet invariant mass.
- Cut 10: $m_{jj[1]} > 15$ GeV and $\Delta R_{jj[1]} > 0.4$, where $m_{jj[1]}$ is the invariant mass of the off-shell-W jet pair, and $\Delta R_{jj[1]}$ is the corresponding ΔR.
- Cut 11: $log_{10} P_W > -5.2$, where P_W is the quantity described previously.
- Cut 12: $m^Z_{jj[0]} < 89$ GeV, where $m^Z_{jj[0]}$ is the invariant mass of the on-shell dijet pair selected to align to the mass of the Z boson.

$Z(l^+l^-)H, H \to W(qq)W(qq)$ Cut Flow

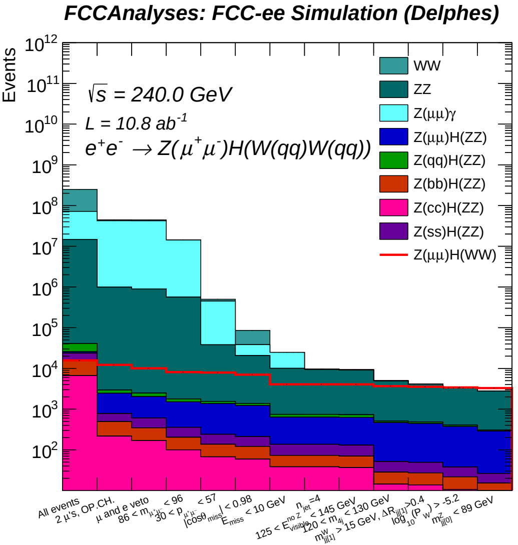

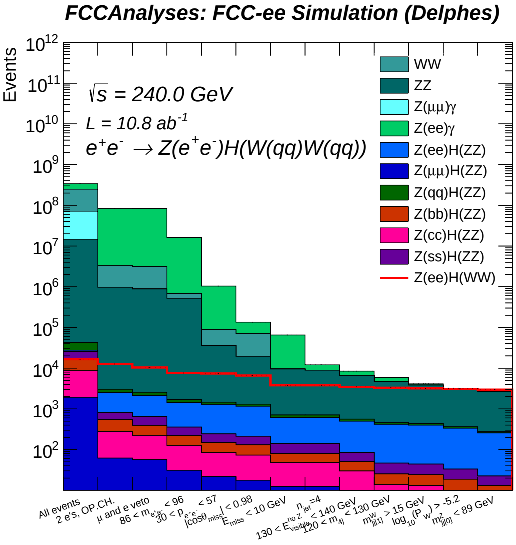

Final Results: Recoil mass after selections

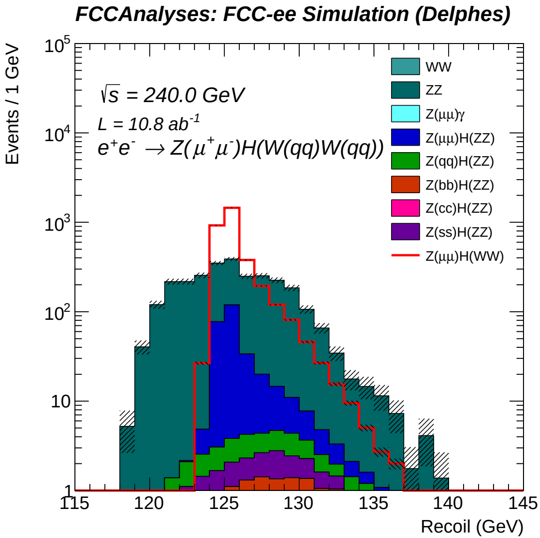

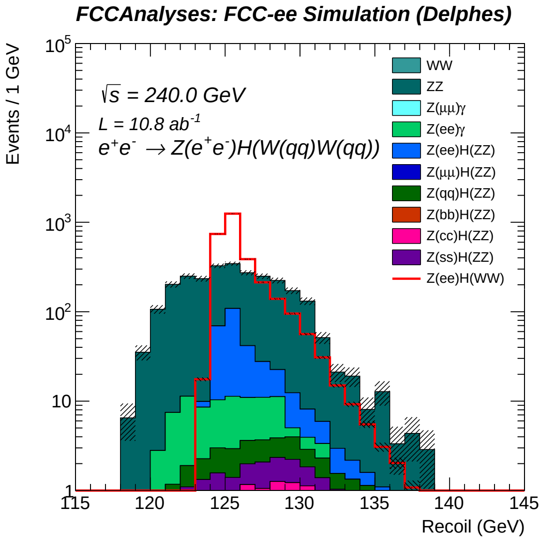

Likelihood Fit to m_{recoil} Results

- We employ the **RooFit**-based *CMS Combine* tool to perform a binned likelihood fit to extract the uncertainty of the *ZH* production.
- The fit is performed on the Recoil Mass distribution.
- All backgrounds are subjected to a 1% log-normal uncertainty, except for the *ZZ* background, which was set at 3%.

Channel	Stat-only	1% norm all BKG	1% norm, 3% HZZ
$\mu\mu$	2.1072	2.1377	2.1512
ee	2.2548	2.2895	2.3020
Combination	1.5395	1.5811	1.5990

Final uncertainty results for the $Z(\ell\ell)H(W_{qq}W_{qq})$ production at $\sqrt{s} = 240$ GeV.

Results in Technical Note (DOI:10.17181/x48j4-3kg84) part of the Future Circular Collider Feasibility Study Report, to be presented to the European Strategy for Particle Physics (ESPP).

Parallel Work: Vector Boson Fusion (VBF)

VBF is a remarkably clean channel for producing the Higgs boson at e^+e^- colliders. (Felipe Martinez's MasterThesis)

$$e^+e^- \to \nu_e\overline{\nu}_e H$$

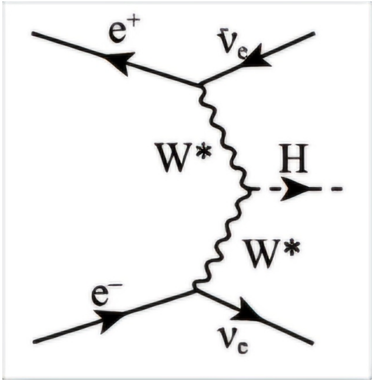

Key Kinematic Signatures:[a]

- **Undetected Neutrinos:** Lead to significant missing transverse energy (E_T^{miss}). This is our primary tag.
- **Forward-going Leptons:** The initial e^+e^- scatter at a small angle.
- **Central Higgs Production:** The Higgs boson is produced with moderate transverse momentum.
- **Decay Products:** In our case, two b-jets from $H \to b\overline{b}$.

[a] [8] Howard Baer et al. The International Linear Collider Technical Design Report Volume 2: Physics. 2013.

VBF: Separating Signal from Background

The primary difficulty in observing the VBF process is the extraction of its faint signal from a much larger background of other physical processes.

- **Signal:** $e^+e^- \to \nu_e\overline{\nu}_e H, H \to b\overline{b}$
- **Major Backgrounds:** ZH, ZZ, WW, and $t\bar{t}$ production, which can mimic the final state.

Simple cuts on single variables are not enough. We need a more powerful tool.

Multivariate Analysis (MVA) uses machine learning to find complex correlations between multiple variables, creating a single, powerful discriminant to separate signal and background events.

Why Boosted Decision Trees (BDT) and XGBoost?

We focus on two state-of-the-art algorithms: BDTs and their advanced implementation, XGBoost.

Boosted Decision Tree (BDT)

- A single decision tree is a simple flowchart.
- A BDT is an **ensemble** of many "weak" trees.
- It learns sequentially: each new tree is trained to correct the mistakes of the previous ones.
- The final result is a powerful, robust classifier.

[a]

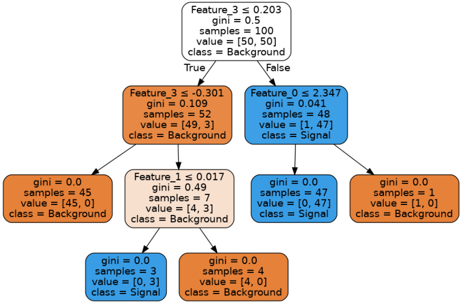

[a] [42] Jerome H. Friedman. Greedy function approximation... *Annals of Statistics*, 2001.
[61] Byron P. Roe, et al. Boosted Decision Trees as an Alternative... *NIM A*, 2005.

A Simple View of Boosted Decision Trees (BDT)

How a Child Learns to Identify a "Dog"

Lesson 1: A Simple Rule

- You give the child a simple rule: *"If it has four legs, it's a dog."*
- **Result:** The child correctly identifies most dogs, but makes mistakes: they also call cats, lions, and cows "dogs".

Lesson 2: Focus on the Mistakes

- You take **only the pictures the child got wrong** (the cats, lions, cows).
- You give a new rule for that pile: *"From this group, if it meows, it's NOT a dog."*
- **Result:** The child now correctly separates the cats. This is the **"boosting"** step: we improve the model by focusing on its errors.

Lesson 3, 4... The Process Repeats

- You take the remaining mistakes (lions, cows) and give another rule: *"From this pile, if it's huge and has horns, it's NOT a dog."*
- Each new lesson is a simple rule targeted at fixing the previous errors.

Final Knowledge: The Ensemble

The child's final, accurate understanding of a "dog" isn't one single rule, but the **combination of all the simple lessons**.

Simulated Samples and MVA Inputs

All samples are normalized to a target integrated luminosity of 3 ab^{-1}.

Simulated Processes at $\sqrt{s} = 365$ GeV

Process	Cross-Section (pb)
Signal ($\nu_e \bar{\nu}_e H \to b\bar{b}$)	**0.02181**
Signal ($\nu_\mu \bar{\nu}_\mu H \to b\bar{b}$)	**0.00481**
BG: ZZ	0.6428
BG: WW	10.7165
BG: tt	0.800
BG: ZH ($\nu\bar{\nu}$)	0.00481

Core Features for MVA Classification

- m_{jj}: invariant mass of the two leading jets.
- E_{miss}: total missing energy.
- p_{miss}: magnitude of missing momentum.
- $\cos\theta_{miss}$: direction of missing momentum.

Key Strategy

The MVA combines these variables into a single score. We can then apply a cut on this score to drastically improve the signal-to-background ratio.

Before BDT Implementation

Sequential Selection Cuts:

- Remove jets containing leptons (e or μ).
- Require exactly two jets in the event.
- Apply an angular cut: $\cos\theta_{miss} < 0.98$.
- Require both jets to pass a b-tagging threshold.
- Apply a di-jet mass window: $|m_{jj} - m_H| \geq 30$ GeV (sideband).
- Require significant missing energy: MET > 15 GeV.

Key Results at $L = 3$ ab^{-1} with $\sqrt{s}$=365 GeV

- Final Event Counts: Signal (S) = 55,094.2 and Background (B) = 136,277.
- This yields a powerful statistical significance: $\sigma = S/\sqrt{B} \approx 125.9$.
- The projected luminosity to achieve a 5σ discovery with this method is remarkably low, only ≈ 4.7 fb^{-1}.

This strong baseline demonstrates the excellent potential of the FCC-ee. The goal of the MVA is to further improve upon this result by exploiting correlations the simple cuts cannot capture.

Event Yields for $L = 3\ \mathrm{ab}^{-1}$ after Final Selection

The MVA cut significantly enhances the signal-to-background ratio.

No MVA score Cut

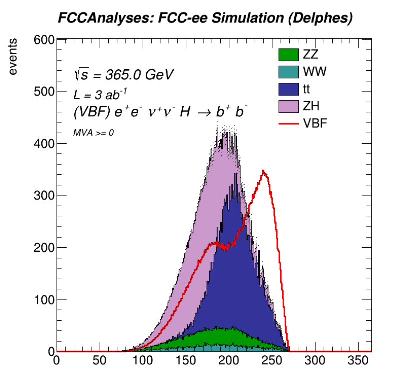

MVA score > 0.5

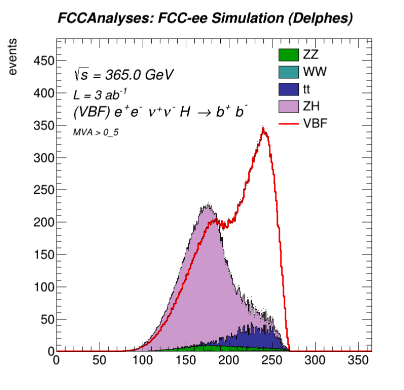

Felipe's Thesis Final Results

Projected Measurement for the VBF Signal Channel

Based on the statistical fit for the optimal selection ('MVA $>$ 0.5'), we project the measurement of the VBF signal cross-section to be:

$$\sigma_{VBF(H\to b\bar{b})} = (26.62 \pm 0.45)\ \text{fb}$$

This corresponds to a remarkable relative precision of approximately **1.52%**.

Context and Comparison: This projected precision of 1.52% is a robust estimate. An internal FCC analysis using a different technique (Neural Networks) on an inclusive sample projects a higher precision of $\pm$0.68%.† Our work serves as a crucial, independent confirmation using a distinct MVA methodology, establishing a solid baseline for this channel.

† [34] Andrea Del Vecchio, et al. Measurement of Higgs boson hadronic decays at FCC-ee, March 2025.

Conclusions

- We have evaluated the **sensitivity of the measurement** of the Higgs boson branching ratio to the hadronic decay mode of the W^+W^- final state at the Future Circular Collider.
- The signal was extracted via a **binned likelihood fit** to the recoil mass distribution, utilizing the Combine tool. The fit was applied across the full range of the recoil mass, with a bin width of 1 GeV.
- The uncertainties in the measured branching ratio for the $H \to W^+W^-$ hadronic decay mode were found to be 2.15 and 2.30 for the $Z(\mu\mu)$ and $Z(ee)$ channels, respectively, with a **combined uncertainty of** 1.60.
- These results highlight the potential of the Future Circular Collider to provide a **precise determination of the Higgs branching ratio** to a pair of W bosons, with minimal uncertainty.

References I

[1] M. Benedikt et al. Future Circular Collider Feasibility Study Report: Volume 1, Physics, Experiments, Detectors. 4 2025. doi: 10.17181/CERN.9DKX.TDH9.

[2] Jan Eysermans and Michele Selvaggi. Total zh hadronic cross-section at fcc-ee and combination with leptonic final states, March 2025. URL https://doi.org/10.17181/e9wsh-tb178.

[3] Jan Eysermans, Gregorio Bernardi, and Li Ang. Higgs boson mass and model-independent zh cross-section at fcc-ee in the di-electron and di-muon final states, March 2025. URL https://doi.org/10.17181/c5dn3-c0s73.

[4] Paolo Azzurri, Gregorio Bernardi, Sylvie Braibant, David d'Enterria, Jan Eysermans, Patrick Janot, Ang Li, and Emmanuel Perez. A special Higgs challenge: measuring the mass and production cross section with ultimate precision at FCC-ee. *Eur. Phys. J. Plus*, 137(1):23, 2022. doi: 10.1140/epjp/s13360-021-02202-4.

[5] A. Abada et al. FCC-ee: The Lepton Collider: Future Circular Collider Conceptual Design Report Volume 2. *Eur. Phys. J. ST*, 228(2):261–623, 2019. doi: 10.1140/epjst/e2019-900045-4.

References II

[6] S. Catani, Yu.L. Dokshitzer, M. Olsson, G. Turnock, and B.R. Webber. New clustering algorithm for multijet cross sections in e+e− annihilation. *Physics Letters B*, 269(3):432–438, 1991. ISSN 0370-2693. doi: https://doi.org/10.1016/0370-2693(91)90196-W. URL https://www.sciencedirect.com/science/article/pii/037026939190196W.

[7] Piotr Niezurawski, Aleksander Filip Zarnecki, and Maria Krawczyk. Study of the higgs-boson decays into w +w − and zz at the photon collider. *Journal of High Energy Physics*, 2002(11):034, dec 2002. doi: 10.1088/1126-6708/2002/11/034. URL https://dx.doi.org/10.1088/1126-6708/2002/11/034.

THANK YOU!

Back-up Slides

Higs Mass Measurement Studies

- The precise measurement of m_H relies on the accurate lepton momentum resolution to resolve the recoil mass distribution.
- Maximum Likelihood Fit with the *Combine* tool.
- Fit to the signal distribution is done through two single-sided Crystal-Ball functions plus a Gaussian.

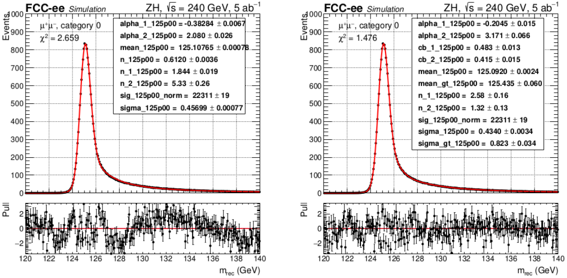

Signal model fit, with a double CB (left) and two CB+Gaussian (right)[‡].

[‡]https://doi.org/10.17181/jfb44-s0d81

Higgs Mass Measurement Studies

- Fits to the signal for variations of ± 50 MeV around $m_H = 125$ GeV were performed, finding that only the means (μ and μ_G) depend on m_H.
- Background is modeled with a third-order Bernstein polynomial.
- **Combined result**: $m_H = 125$ GeV $\pm\, 3.07$ MeV.

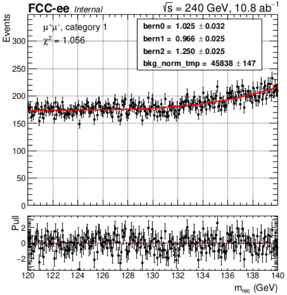

Background model fit with a third-order Bernstein polynomial§.

§https://doi.org/10.17181/jfb44-s0d81

CMS Combine Tool

The *CMS Combine* tool helps build likelihood models for binned and unbinned data, perform statistical tests on the fit and provides tools for validation of the statistical analysis.
Likelihood for Binned Data:

$$\mathcal{L}_{bin}(\vec{\Phi}) = Poiss(n_{obs}; n_{exp}(\vec{\Phi})) \tag{4}$$

$$\mathcal{L}_{primary} = \prod_{bins} \mathcal{L}_{bin} \tag{5}$$

Likelihood for Unbinned Data:

$$\mathcal{L}_{data} = Poiss(n_{obs}; n_{exp}(\vec{\Phi})) \prod_{i}^{N_{obs}} pdf(\vec{x_i}; \vec{\Phi}) \tag{6}$$

Missing momentum direction: θ_{miss}

Additional cut is applied to further reduce Z/γ events, which typically contain hard ISR photons collinear to the beam and therefore left undetected, resulting in a peaking behavior of the direction of the missing momentum vector towards the forward regions.

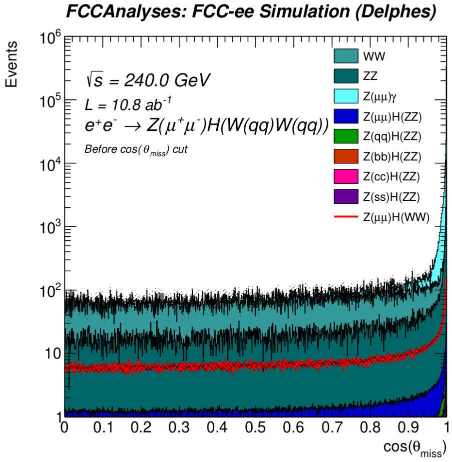

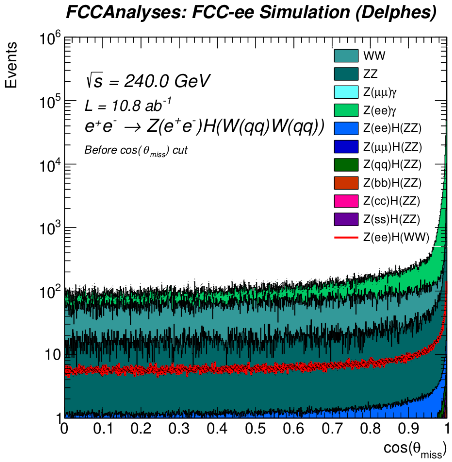

Visible energy without the Z $\ell\ell$'s: $E_{visible}^{\text{no Z}}$

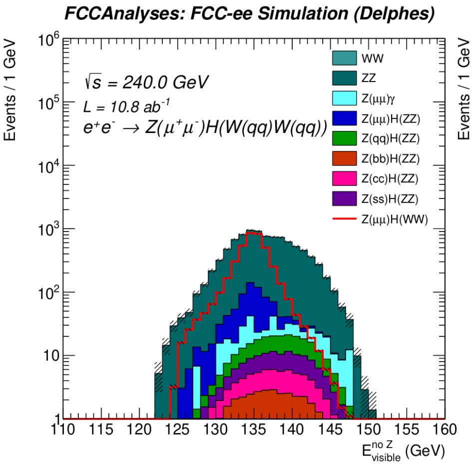

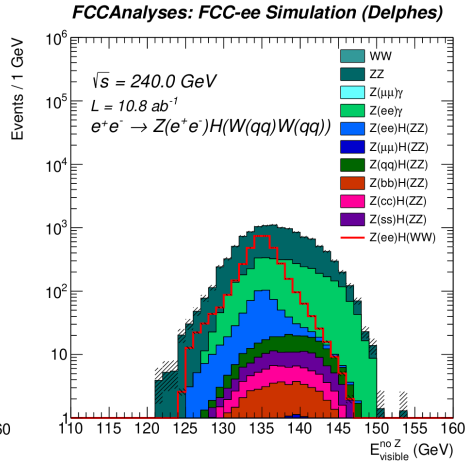

4-jet invariant mass: m_{4j}

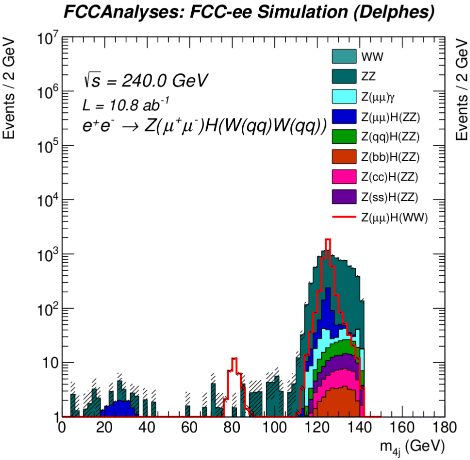

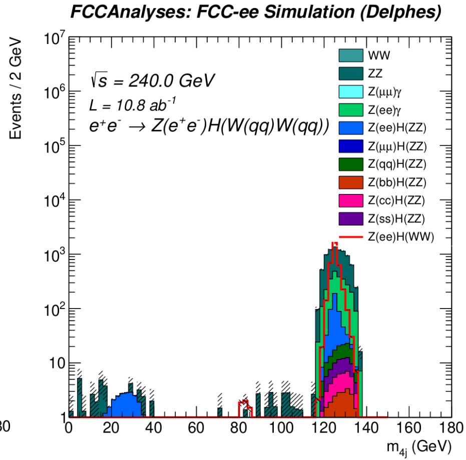

"*Off-shell*" W-dijet mass: $m^{W}_{jj[1]}$

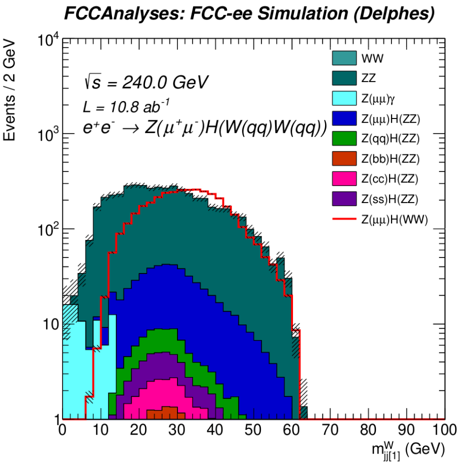

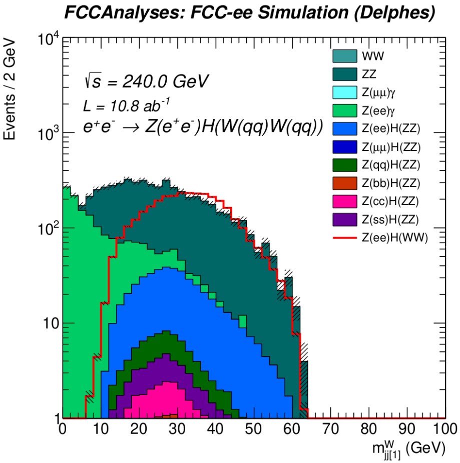

"*On-shell*" Z-dijet mass: $m^{Z}_{jj[0]}$

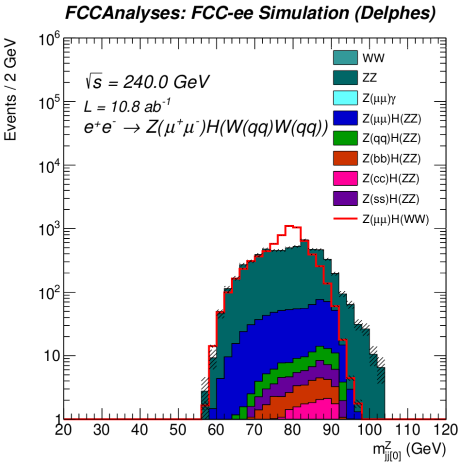

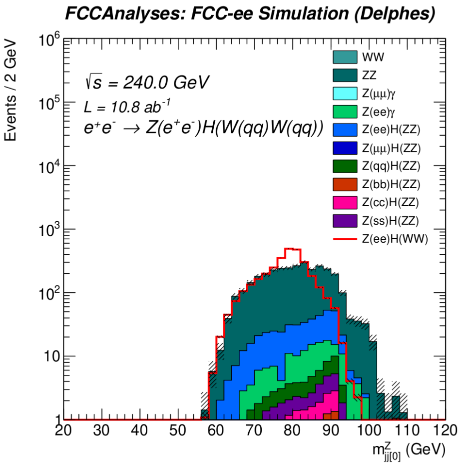

Multivariate Analysis and BDT training

The classification of signal events in the $Z(\ell\ell)H, H \rightarrow WW$ process at FCC-ee is performed using a Multivariable Analysis (MVA) approach based on Boosted Decision Trees (BDT), implemented via the XGBoost library.

Features:

- **Four-jet invariant mass:** *jj_m_4jet*,
- **On-shell-W dijet invariant mass:** *jj_m_ww_1*,
- **Off-shell-W dijet invariant mass:** *jj_m_ww_2*,
- **Probability of dijet pairings to correspond to the W boson:** *PW* ,
- **On-shell-Z dijet invariant mass:** *jj_m_zz_1*,
- **Off-shell-Z dijet invariant mass:***jj_m_zz_2*
- $Z_{\mu\mu}$ **kinematics:** momentum (*zmumu_p*) and $\Delta\phi$ (*zmumu_deltaphi*).
- **Visible energy (excluding Z muons):** *visible_energy*.
- **On-shell-W and Off-shell-W dijet pairs separation:** ΔR_1 (*DeltaR_1*), ΔR_2 (*DeltaR_2*), respectively.

Hyperparameters:

- `objective`: `binary:logistic`
- `eval_metric`: `auc`
- `eta`: 0.1
- `max_depth`: 5
- `subsample`: 0.5
- `colsample_bytree`: 0.5
- `n_estimators`: 350
- `learning_rate`: 0.20
- `gamma`: 3
- `min_child_weight`: 10
- `early_stopping_rounds`: 25

BDT variable scores

Scores for each of the features chosen for the clasifier in the BDT training. A higher score suggests that the variable is more valuable for classification purposes.

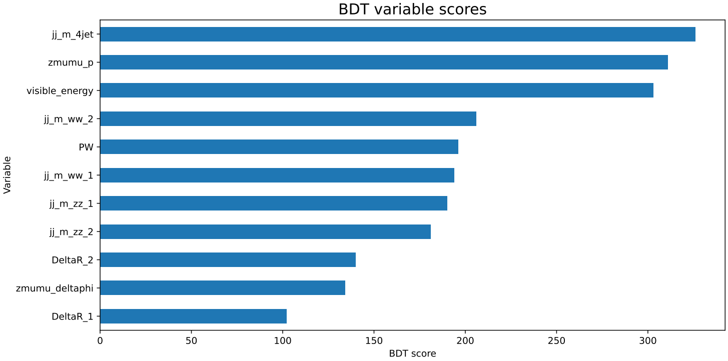

ROC Curve

Receiver Operating Characteristic (ROC) curve. In our case, the value of the Area Under the Curve (AUC) indicates that the ability of the model to distinguish between signal and background is acceptable (above 0.9).

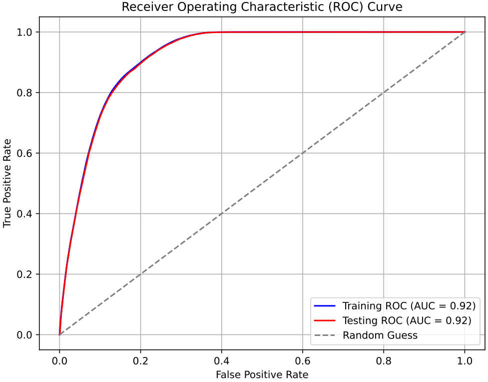

BDT Score Distribution

Distribution of the scores produced by the BDT classifier for the signal (blue) and background (red).